Characterization of Oxygen-Induced Retinopathy in Mice Carrying an Inactivating Point Mutation in the Catalytic Site of ADAM15

Thorsten Maretzky,[1] Carl P. Blobel,[1,2] and Victor Guaiquil[3]

[1]Arthritis and Tissue Degeneration Program, Hospital for Special Surgery, New York, New York, United States
[2]Departments of Medicine and of Physiology, Biophysics and Systems Biology, Weill-Cornell Medical College of Cornell University, New York, New York, United States
[3]The Margaret M. Dyson Vision Research Institute, Department of Ophthalmology, Weill-Cornell Medical College of Cornell University, New York, New York, United States

Correspondence: Victor Guaiquil, Margaret M. Dyson Vision Research Institute, Department of Ophthalmology, Weill-Cornell Medical College, 1300 York Avenue, New York, NY 10065, USA; vig2002@med.cornell.edu.

Submitted: March 28, 2014
Accepted: September 12, 2014

Citation: Maretzky T, Blobel CP, Guaiquil V. Characterization of oxygen-induced retinopathy in mice carrying an inactivating point mutation in the catalytic site of ADAM15. *Invest Ophthalmol Vis Sci*. 2014;55:6774–6782. DOI:10.1167/iovs.14-14472

Purpose. Retinal neovascularization is found in diseases such as macular degeneration, diabetic retinopathy, or retinopathy of prematurity and is usually caused by alterations in oxygen supply. We have previously described that mice lacking the membrane-anchored metalloproteinase ADAM15 (a Disintegrin and Metalloprotease 15) have decreased pathological neovascularization of the retina in the oxygen-induced retinopathy (OIR) model. The main purpose of the present study was to determine the contribution of the catalytic activity of ADAM15 to OIR.

Methods. To address this question, we generated knock-in mice carrying an inactivating Glutamate to Alanine (E>A) point mutation in the catalytic site of ADAM15 (*Adam15E>A* mice) and subjected these animals to the OIR model and a heterotopic tumor model. Moreover, we used cell-based assays to determine whether ADAM15 can process cell surface receptors involved in angiogenesis.

Results. We found that pathological neovascularization in the OIR model in *Adam15E>A* mice was comparable to that observed in wild type mice, but tumor implantation by heterotopically injected melanoma cells was reduced. In cell-based assays, overexpressed ADAM15 could process the FGFR2iiib, but was unable to process several receptors with roles in angiogenesis.

Conclusions. Collectively, these results suggest that the catalytic activity of ADAM15 is not crucial for its function in promoting pathological neovascularization in the mouse OIR model, most likely because of the very limited substrate repertoire of ADAM15. Instead, other noncatalytic functions of ADAM15 must be important for its role in the OIR model.

Keywords: retina, ADAM15, angiogenesis, knock-in, tumor model

Pathological neovascularization is one of the leading causes of blindness in humans, and is found in diverse eye diseases, including diabetic retinopathy, macular degeneration, and retinopathy of prematurity.[1–3] Moreover, it can contribute to other pathologies, such as cancer and rheumatoid arthritis.[4,5] Several members of the ADAM (a Disintegrin and Metalloprotease) family of membrane-anchored metalloproteinases, such as ADAM8,[6] ADAM9,[7] ADAM15,[8] and ADAM17,[9] have been found to play critical and distinct roles in pathological neovascularization. Absence of ADAM9, ADAM15, or ADAM17 reduces revascularization of the retinal capillary bed in mice subjected to the oxygen-induced retinopathy (OIR) model.[10–12] In addition, these knockout mice develop smaller tumors when injected heterotopically with a cancer cell line. However, *Adam8–/–* mice showed increased revascularization of the central avascular area of the retina in the OIR model and had larger tumors compared to controls, consistent with a role for ADAM8 in limiting neovascularization. ADAM15 has been implicated in various disease conditions, including cancer, atherosclerosis, rheumatoid arthritis, and osteoarthritis.[8,13–19] The multidomain structure of ADAM15 consists of a catalytically active metalloprotease domain, a disintegrin domain and cysteine rich region, which may mediate cell–cell or cell–matrix interactions, and the cytoplasmic domain, which may have a role in signaling or intracellular transport.[20–23] ADAM15, as well as several other ADAMs, are able to shed the ectodomains of membrane bound receptors, a process that is mediated by the catalytic site of the metalloprotease domain and that is fundamental for cellular communications.[24–33] ADAM15 contains a catalytic site consensus sequence for zinc-dependent metalloproteases (HEXXH), and purified recombinant ADAM15 is catalytically active.[34]

Previously, ADAM15 was found to be highly expressed in endothelial cells during mouse development and to have a role in promoting pathological retinal neovascularization.[8] The main goal of the current study was to determine whether the catalytic activity of ADAM15 is important for its role in promoting pathological neovascularization in vivo. Therefore, we developed a knock-in mouse carrying an inactivating point mutation in the catalytic site of ADAM15 (HEXXH > HAXXH)[35]

and evaluated ocular neovascularization by subjecting these animals to the OIR model of retinopathy of prematurity and the heterotopic injection of cancer cells. Moreover, we determined whether overexpressed ADAM15 is able to process cell surface receptors with known roles in angiogenesis and neovascularization.

Materials and Methods

Reagents

All chemicals and reagents were purchased from Sigma-Aldrich Corp. (St. Louis, MO, USA), unless indicated otherwise. FITC-Isolectin B4 was purchased from Vector Labs (Burlingame, CA, USA), anti-CD31 was from BD Biosciences/Pharmingen (San Diego, CA, USA), and anti-rat Cy3 from Jackson Immunoresearch (West Grove, PA, USA); the anti-ADAM15 monoclonal antibody used for Western blot have been previously described.[36,37]

Construct Design

The complete coding region of ADAM15 contained in a cosmid was subcloned into fragments and partially sequenced to find the metalloprotease domain using the ADAM15 genomic sequence as a template (GenBank accession number AB022089). When the cosmid was digested with *Kpn*I, a 4.8-Kb fragment was released that was subcloned into pBSK+. The plasmid containing the insert was used to introduce a point mutation in the catalytic site of the metalloprotease domain (change of adenine to cytosine at position 6829 of AB022089 using the QuickChange XL site directed mutagenesis kit, Stratagene, La Jolla, CA, USA) that led to an E>A mutation and corresponding inactivation of the catalytic site.[35] Additionally, an *Asc*I site was created by mutating intronic positions 7014 and 7017, allowing the insertion of a neomycin selectable marker flanked by *Frt* sites. The plasmid was digested with *Kpn*I, and the released fragment containing the mutated catalytic site plus the neomycin marker was ligated into a pBADT3-BSKII plasmid that contains an actin-driven diphtheria toxin for negative selection. This final ADAM15 targeting construct was used to generate targeted embryonic stem (ES) cells (Fig. 1A). Correct integration of the targeting construct was confirmed by Southern blot using a neo specific probe (Fig. 1B).

Generation of Mice With a Catalytically Inactive ADAM15

ES cells carrying a properly targeted ADAM15E>A allele were injected into blastocysts from C57BL/6J mice in order to generate chimeric offspring. The resulting chimeric male mice with a high percentage of the agouti coat color (indicating a high degree of chimerism) were mated with C57BL/6J females. The offspring from these crosses were mated with C57B6;SJL-Tg(ACTFLPe)9205Dym/J mice (*FLP1* recombinase +, Jackson Labs, Bar Harbor, ME, USA) to excise the neo cassette, which was flanked by *Frt* sites in the targeted allele. The resulting *Adam15E>A* offspring were later crossed with mixed background (129/SvJ/C57BL/6J) mice to generate breeding pairs of 129/SvJ/C57BL/6J mixed genetic background for this study and for comparison with the *Adam15*–/– mice, which were also of 129/SvJ/C57BL/6J mixed genetic background. The *Adam15E>A* mice were genotyped by PCR using the following set of primers that amplify a region that contains the mutation of the catalytic site of ADAM15; forward primer 5′ CGTTGCCTCCTCGATT GCCCATGC 3′; reverse primer 5′ ATCTGGGAAGCCACAGT CAC 3.′ The products of the PCR correspond to a 408-bp band for the wild type (WT) animals and a 510-bp band for *Adam15E>A* mice (Fig. 1C).

Evaluation of Neovascularization After OIR

All animal work was performed following the guidelines of the American Veterinary Association and was approved by the Institutional Animal Care and Use Committee of the Hospital for Special Surgery in accordance with the ARVO Statement for the Use of Animals in Ophthalmic and Vision Research. The response of WT, *Adam15*–/– and homozygous mutant *Adam15E>A* mice (referred to as *Adam15E>A* throughout) to relative hypoxia was assessed by using the OIR model as described previously.[3,36,38,39] Since the animals were of mixed genetic background (129/SvJ/C57BL/6J, see above), all experiments were performed by comparing *Adam15*–/– or *Adam15E>A* with their respective WT littermates that were offspring from heterozygous parents (*Adam15*+/– or *Adam15E>A*+/–). Briefly, for the OIR model,[40,41] post natal day 7 (P7) mice along with their nursing mother were exposed to 75% oxygen until P12, then returned to normal room air. At P17 the mice were euthanized and both eyes were removed and fixed in 4% paraformaldehyde (PFA) overnight at 4°C. Quantitation of neovascularization was performed on 6-μm sections of paraffin embedded retinas stained with hematoxylin and eosin. The endothelial cell nuclei that were present on the vitreal side of the internal limiting membrane were counted in five sections on each side of the optic nerve, 30 to 90 μm apart, as previously described.[36] The number of tufts per retina was determined by counting only tufts that were clearly visible on retina flat mounts at 4× magnification as described.[6] The hyperoxia-induced avascular area that develops in the retinas of OIR-treated mice and the tortuosity of the major central vessels of the retina were evaluated in flat mounted retinas stained with FITC-labeled isolectin B4 at P17 as described.[10] The sizes of the avascular area and of the total retina were outlined using ImageJ software (National Institutes of Health, Bethesda, MD, USA), and the resulting values were used to calculate the percentage of the avascular area relative to the total retina area.[10] The tortuosity index in the major vessels of the retina was quantified by tracing a line along the tortuous vessel and comparing it to a straight line, traced from its origin on the optic nerve to the first point of branching.[42] The unpaired Student's *t*-test (equal variance, two sided) was used to evaluate the statistical significance of the observed differences between *Adam15*–/–, *Adam15E>A*–, and their respective WT control mice, with $P < 0.05$ considered to be significant (*).

Evaluation of Tumor Size and Implantation

To determine whether the inactivation of the catalytic site of ADAM15 affects a different angiogenic model and mimics the effect on tumor development that was previously observed in *Adam15*–/– mice,[8] we generated litters of *Adam15*–/– mice and their WT controls, or *Adam15E>A* mice and their WT controls as follows. Initially we collected *Adam15E>A* and WT offspring from one set of heterozygous *Adam15E>A*+/– parents, and then mated either *Adam15E>A*–/– mice with one another, or their WT littermates with one another to generate litters that were all *Adam15E>A*–/– or WT, but highly related because their *Adam15E>A*–/– or WT parents were littermates; that is, they were derived from the same heterozygous grandparents. To evaluate tumor development and implantation, age- and sex-matched animals were subcutaneously injected with 1×10^6 B16F0 mouse melanoma cells resuspended in PBS. The mice in each experiment were euthanized at the same time, between 2 and 3 weeks after injection, and the tumors were removed and weighed. The

Investigative Ophthalmology & Visual Science

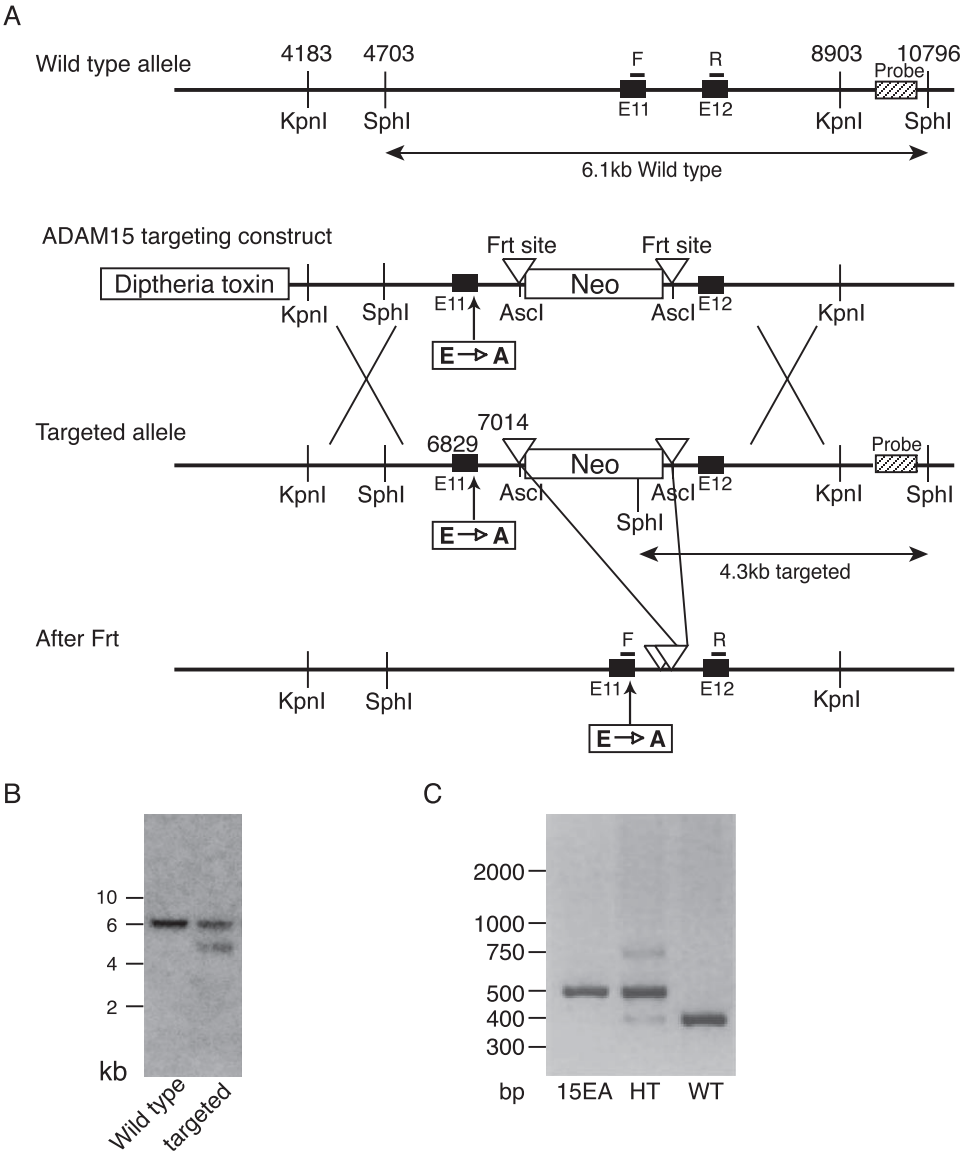

Figure 1. Targeted inactivation of the catalytic site of ADAM15 in mice. (**A**) Schematic representation of the WT allele of mouse ADAM15 indicates the *Kpn*I restriction sites used to generate the plasmid construct. The targeting construct shows the insertion of a diphtheria toxin gene cassette that was added at the 5′ end to select against nonhomologous recombination events. A pMC1neoPolyA cassette flanked by *Frt* sites was inserted in the newly created *Asc*I restriction site. A mutation of $a > c$ at position 6829 of the genomic ADAM15 sequence (GenBank accession number AB022089) introduced the inactivating H**E**LGH > H**A**LGH mutation in the catalytic domain of ADAM15 and also generated a new *Nsi*I site that allowed screening for the *Adam15E>A* mutation using genomic DNA. The bottom scheme shows the targeted allele where the neo cassette is removed after *Frt* recombination, leaving an additional 100 nucleotides in the intronic region used to insert the neo gene. (**B**) The targeting allele was screened by Southern blot using a specific probe designed to detect the neo gene. The 749-bp probe was gel purified and recognized a 6.1-Kb fragment (WT allele) of *Sph*I digested genomic WT DNA and a 4.3-Kb fragment (targeted allele) in the E>A mutant as shown in the Southern blot. (**C**) Mouse genotyping was confirmed by a PCR reaction that detects a difference in the size of the amplified fragments between the WT and the *Adam15*E>A allele (15EA), using the primers described in Material and Methods. The PCR primers bind to exons 11 and 12 and are depicted in the WT and knock in alleles (F, forward primer; R, reverse primer). HT, heterozygous.

normalization of the results of the tumor model for comparison between different experiments was performed as described previously.[10,36] To determine tumor implantation, those mice having tumors of 0.05 g or more were considered as successfully implanted and those with smaller tumors were considered as failed implantation and included in the analysis. The unpaired Student's *t*-test (equal variance, two sided) was used for statistical evaluation, with $P < 0.05$ considered statistically significant.

Evaluation of ADAM15 Catalytic Activity Using Cell-Based Protein Ectodomain Shedding Assays

Shedding of membrane-associated receptors was evaluated in mouse embryonic fibroblasts (mEFs) transfected with either a plasmid-containing WT ADAM15 or the catalytically inactive ADAM15E>A, respectively, along with candidate membrane-anchored alkaline phosphatase-tagged substrate proteins, as described.[43] We evaluated the release of alkaline-phosphatase-tagged FGFR2iiib, CD40, VCAM, EphB2, EphB4, P-selectin,

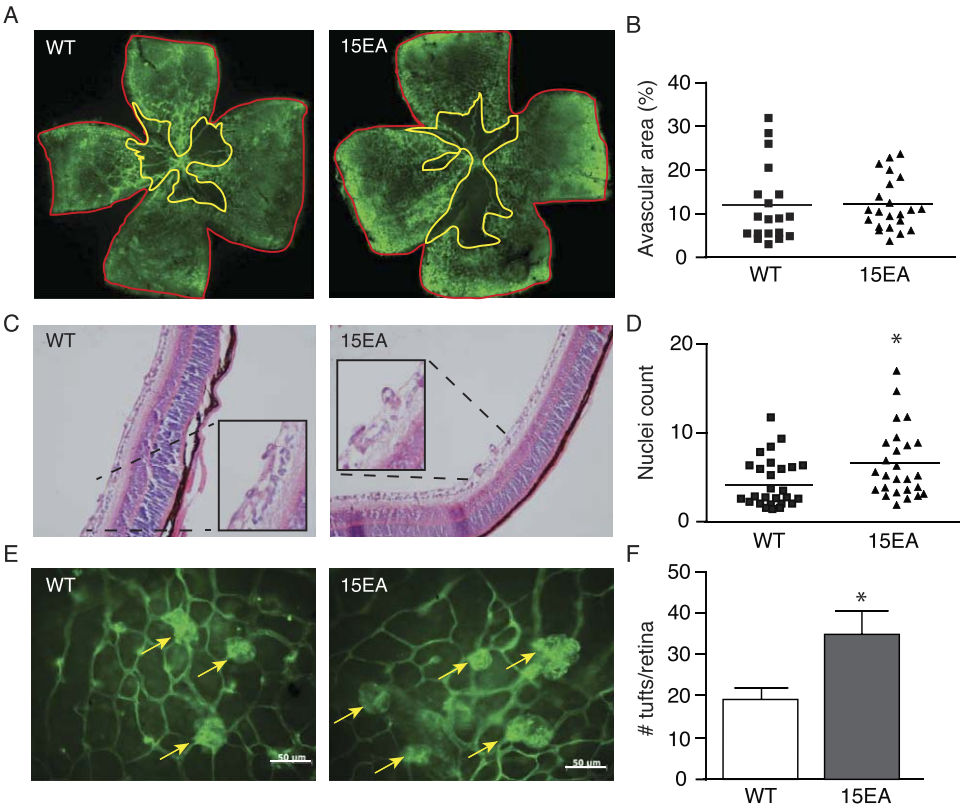

Figure 2. Revascularization response in *Adam15E>A* mice exposed to OIR. *Adam15E>A* and their respective WT control mice were subjected to the OIR model (see Materials and Methods for details). **(A)** Representative whole mount FITC-isolectinB4-stained retinas of WT and *Adam15E>A* mice showing the avascular area at P17 in yellow. **(B)** Quantification showed that *Adam15E>A* mice had no significant change in the size of the central avascular area compared to their WT littermate controls (WT mean = 14.7 ± 2.4 SEM, $n = 19$; E>A mean = 14.9 ± 1.5 SEM, $n = 22$, $P = 0.47$). **(C–F)** Further analysis showed a significant difference in the number of vascular cell nuclei on the vitreal side of the internal limiting membrane **(C, D)** and of tufts that contributed to pathological neovascularization **(E, F)** in *Adam15E>A* mice compared to WT littermate controls (WT mean = 4.5 ± 0.5 SEM, $n = 27$; E>A mean = 6.6 ± 0.8 SEM, $n = 26$, $P = 0.026$ for nuclei and $P = 0.011$ for tufts), each point in panel **(D)** represents the average number of nuclei per section of one animal. Arrows in E indicate retinal tufts. Asterisk indicates $P < 0.05$ using Student's *t*-test.

Tie2, VE-cadherin, and VEGFR2.[7,9,43,44] Alkaline phosphatase shedding assays were performed as described previously.[37,43,45] As a positive control for shedding of the candidate substrates, transfected cells were stimulated with phorbol 12-myristate 13-acetate (PMA), which is a strong activator of ADAM17-dependent shedding, or with ionomycin, which strongly induces ADAM10 and ADAM17 dependent shedding.[45–48]

Results

Targeted Inactivation of the Catalytic Site of ADAM15 in Mice

In order to determine the role of the catalytic activity of ADAM15 in oxygen-induced retinal neovascularization in mice, we introduced an inactivating point mutation in the catalytic site of the ADAM15 metalloprotease domain (H**E**LGH > H**A**LGH, referred to as ADAM15E>A) (Fig. 1, see Materials and Methods for details). When *Adam15E>A*+/– heterozygous mice of mixed genetic background (129/SvJ;C57BL/6J) were mated, the genotype of the offspring followed a normal Mendelian distribution pattern. The homozygous mutant *Adam15E>A* mice were viable and fertile, had no evident spontaneous pathological phenotypes, and were indistinguishable from their WT littermates in appearance, behavior when handled, weight gain after birth, and average weight as adults (data not shown).

Response of *Adam15E>A* to OIR

To determine if the previously documented reduced pathological revascularization of the retina in *Adam15–/–* mice subjected to the OIR model was dependent on its catalytic activity, we exposed *Adam15E>A* mice and their respective WT littermates to the OIR mouse model. At the end of the OIR model at P17, whole mounted retinae were stained with FITC labeled isolectin B4 to visualize endothelial cells and measure the size of the central avascular area (Fig. 2A, see materials and methods for details). We found no significant difference in the size of the central avascular area in *Adam15E>A* mice compared to their WT control littermates (Fig. 2B, WT: $n = 19$, E>A: $n = 22$). Further analysis of cross-sections of the retina and FITC-isolectin B4-stained retina flat mounts showed that there was a significant increase in the number of endothelial cell nuclei on the vitreal side of the internal limiting membrane and of the number of tufts present in retinas in *Adam15E>A* mice compared to their WT littermate controls (Figs. 2C–F, WT: $n = 27$, E>A: $n = 26$).

When we analyzed the tortuosity of the major central vessels at the end of the OIR model at P17, which is considered an indicator for aggressive retinopathy of prematurity in humans,[42] we found that the tortuosity index was similar in

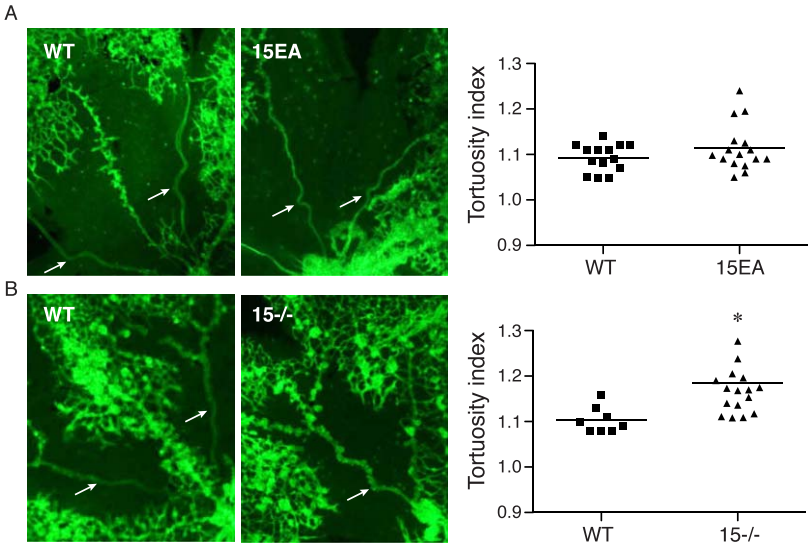

Figure 3. Analysis of vascular tortuosity in *Adam15E>A* and *Adam15–/–* mice after OIR. The FITC-isolectinB4-stained flat mounted retinas of OIR-treated *Adam15E>A*, *Adam15–/–*, and their corresponding WT control mice were evaluated for signs of tortuosity of the major central vessels at the end of the OIR model at P17 (see Materials and Methods for details). (**A**) Vessel tortuosity, which is considered an indicator for aggressive retinopathy, was similar in *Adam15E>A* mice when compared to their WT littermates (WT mean = 1.09 ± 0.01 SEM, $n = 14$; E>A mean = 1.11 ± 0.01 SEM, $n = 16$, $P = 0.09$), (**B**) but was increased in *Adam15–/–* mice compared to controls (WT mean = 1.1 ± 0.01 SEM, $n = 8$; n 15–/– mean = 1.16 ± 0.01 SEM, $n = 16$, $P = 0.0012$). Asterisk indicates $P < 0.05$ in a Student's *t*-test.

Adam15E>A when compared to their WT littermates (Fig. 3A), whereas it was increased in *Adam15–/–* mice (Fig. 3B). Taken together, these finding indicate that inactivation of the catalytic activity of ADAM15 in mice does not lead to decreased pathological neovascularization or increased vascular tortuosity at the conclusion of the OIR model, although tuft formation was significantly increased compared to controls. Thus the *Adam15E>A* mice responded differently than *Adam15–/–* mice when subjected to this mouse model for retinopathy of prematurity.

Reduced Tumor Size and Decreased Tumor Implantation in *Adam15E>A* Mice

A second model in which neovascularization has a prominent role and that allows evaluating the function of the catalytic activity of ADAM15 in mice is to monitor the implantation and development of tumors from heterotopically injected B16F0 melanoma cells. We found a significantly reduced tumor size in *Adam15E>A* mice compared to their WT controls injected with the same number of melanoma cells in an identical volume of PBS (Fig. 4A, WT: $n = 25$, *15E>A*: $n = 25$, see Materials and Methods for details). The analysis of tumors in *Adam15–/–* mice, injected under the same conditions and at the same time, also resulted in smaller tumor sizes compared to their WT controls (Fig. 4B, WT: $n = 35$; *Adam15–/–*: $n = 31$). Further analysis also showed that tumor implantation was reduced in both *Adam15E>A* and *Adam15–/–* mice compared to their respective controls in terms of the number of mice with tumors with a mass equal or above 0.05 g. We found that only 37.5% of the *Adam15E>A* mice injected with B16F0 tumor cells developed detectable tumors, whereas 70.6% of their WT littermates had tumors larger than 0.05 g (Fig. 4C). Under identical conditions, only 54% of *Adam15–/–* mice developed tumors compared to 75.6% of WT controls (Fig. 4D). Overall, our analysis of this heterotopic tumor model in both *Adam15E>A* and *Adam15–/–* mice showed that they not only developed fewer tumors than their respective WT controls, but also that the average tumor weight was significantly lower.

Selective Shedding of Membrane Receptors by ADAM15 in Cell-Based Assays

ADAM15 is known to be catalytically active and to function as a membrane-anchored protease[46,49] that can cleave and release the extracellular domain of a small number of membrane proteins.[50] We therefore hypothesized that ADAM15 could affect pathological neovascularization in endothelial cells by processing membrane proteins with roles in angiogenesis. To address this possibility, we overexpressed several membrane-anchored receptors with critical functions in angiogenesis (CD40, VCAM, EphB2, EphB4, P-selectin, Tie2, VE-cadherin, and the VEGFR2) together with ADAM15 in mEFs. Each candidate substrate contained an alkaline phosphatase tag attached to its ectodomain, which was used to measure the release of these membrane proteins into the culture supernatant.[43,51] The catalytically inactive ADAM15E>A mutant was separately cotransfected along with each substrate and served as a control to monitor baseline shedding by endogenous sheddases in mEFs. Overexpression of ADAM15 increased the shedding of the FGFR2iiib only, but failed to increase the shedding of the other substrates tested here compared to controls overexpressing the catalytically inactive ADAM15E>A (Fig. 5). The shedding of these substrates could be enhanced by treatment with PMA, which activates ADAM17-dependent shedding, or with ionomycin, which activates both ADAM10 and ADAM17.[45–48] These results demonstrate that ADAM15 has an overall very limited substrate repertoire, consistent with the notion that other noncatalytic domains of ADAM15 are important for its function, at least in the OIR model.

Discussion

Previous studies have shown that ADAM15 is highly expressed in endothelial cells during early mouse development and in neovascular tufts in the retina of mice subjected to the OIR

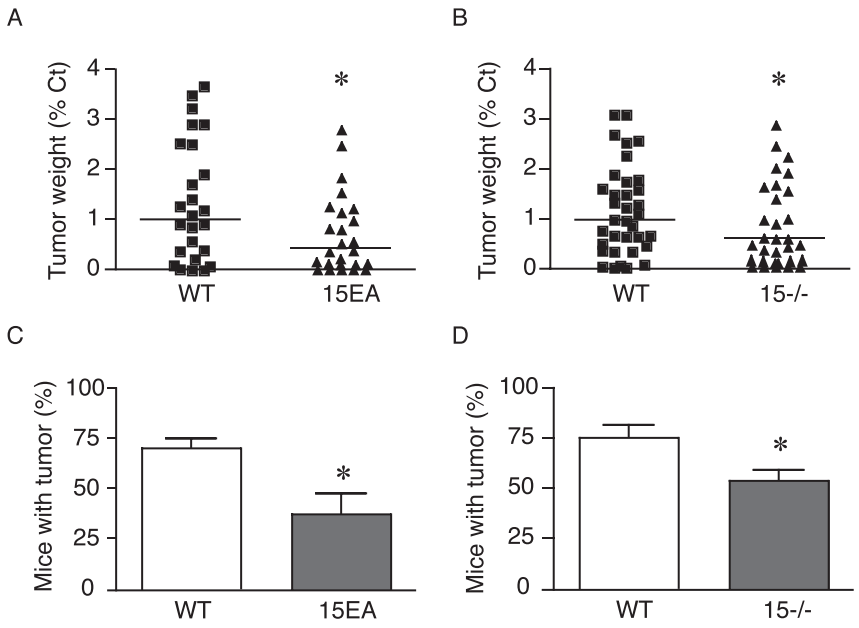

Figure 4. Decreased tumor implantation and development in *Adam15E>A* and *Adam15–/–* mice. Tumor development from 1×10^6 B16F0 melanoma cells injected into the flanks of *Adam15E>A*, *Adam15–/–*, and their corresponding WT controls. To standardize the variations in tumor weight between different experiments, the average tumor weight in WT mice in each experiment was set to 1, and the tumor weight of individual WT and *Adam15E>A* or *Adam15–/–* mice was calculated as a ratio to the average tumor size in their respective WT controls. (**A**) There was a 60% reduction in the average weight of tumors that developed in *Adam15E>A* mice compared to WT controls (n WT = 25, n 15E>A = 25, $P = 0.0012$). (**B**) *Adam15–/–* mice also developed tumors of significantly lower weight than their WT controls (45% reduction; n WT = 35, n *Adam15–/–* = 31, $P = 0.0012$). (**C**) Analysis for tumor implantation showed that in seven experiments, only 37.5% of *Adam15E>A* mice injected with tumor cells developed tumors of $\geq$ 0.05 g in mass compared to 70.6% of WT mice ($P = 0.0064$), indicating that tumor implantation failed in over 60% of *Adam15E>A* mice. (**D**) Similar analysis demonstrated that in nine independent experiments, only 54% of *Adam15–/–* mice injected with tumor cells developed a tumor above the set value, compared to 75.6% of WT controls ($P = 0.0078$).

model.[11,36] Moreover, *Adam15–/–* mice showed a decreased neovascular response in the OIR model compared to WT mice, indicating that ADAM15 plays a critical role in pathological neovascularization. Since ADAM15 is a membrane-anchored metalloproteinase,[34,52] we decided to evaluate whether its catalytic activity is required for its role in pathological neovascularization in vivo. Therefore, we generated knock-in mice carrying a single point mutation (H**E**LGH > H**A**LGH) in the active site of ADAM15 that exchanges the catalytic glutamate with an alanine residue, thereby rendering the enzyme catalytically inactive.[35] The resulting *Adam15E>A* mice were exposed to two models for pathological neovascularization, the OIR model and heterotopic injection of tumor cells. Additionally, we evaluated the catalytic activity of ADAM15 in gain of function (overexpression) assays to determine if ADAM15 can shed the ectodomain of receptors involved in angiogenesis.

The newly generated *Adam15E>A* knock-in mice were comparable to *Adam15–/–* mice in that they appeared healthy, were fertile, and did not show any evident pathological phenotype. When the *Adam15E>A* mice were subjected to the OIR model, they showed a similar revascularization of the central avascular area as the WT controls. However, unlike *Adam15–/–* mice, which had a reduction in the number of endothelial cells that crossed the internal limiting membrane in the OIR model,[36] there was a slight increase in tuft formation and in the number of endothelial cells that had traversed the internal limiting membrane in *Adam15E>A* mice. Finally, the vascular tortuosity of the central retinal vessels, an indicator for the severity of retinopathy of prematurity, was increased in *Adam15–/–* mice compared to controls, but was comparable in *Adam15E>A* mice. Hence, the presence of a catalytically inactive ADAM15 has a different effect on the OIR-induced neovascularization response than the complete inactivation of ADAM15. These results indicate that the loss of other functions of ADAM15 that are not related to its catalytic activity are responsible for the decreased pathological neovascularization observed in *Adam15–/–* mice exposed to the OIR model. Moreover, the observation that tuft formation was increased in *Adam15E>A* mice compared to controls, but decreased in *Adam15–/–* mice,[8] and that vascular tortuosity was increased in *Adam15–/–* mice compared to controls, but not in *Adam15E>A* mice provides additional evidence for differential contributions of the catalytic activity of ADAM15 to these processes. However, in the heterotopic tumor injection model, we observed reduced tumor implantation and development in the *Adam15E>A* and in the *Adam15–/–* mice, in agreement with previous reports describing smaller tumors in *Adam15–/–* mice injected with melanoma cells.[8,19] Thus the catalytic activity of ADAM15 appears to be important for heterotopic tumor development.

Our "gain of function" overexpression experiments to determine the number of target substrates that ADAM15 could shed from cells failed to uncover new substrates among a pool of selected receptors that have a role in angiogenesis. It is interesting to note that other ADAMs, such as ADAM8 and ADAM9, are also highly expressed in neovascular tufts and, unlike ADAM15, have a broad shedding capacity in cell-based assays.[6,7] So the high expression of ADAM15 in the OIR model and its role in neovascularization suggest that these functions are supported by other domains of ADAM15 besides the metalloprotease domain, such as the disintegrin-domain and cysteine-rich region, or its cytoplasmic domain. The intracellular domain of ADAM15 contains SH3 ligand-binding domain that can interact with Src and other SH3-domain containing proteins.[53–56] In this context it is interesting to note that

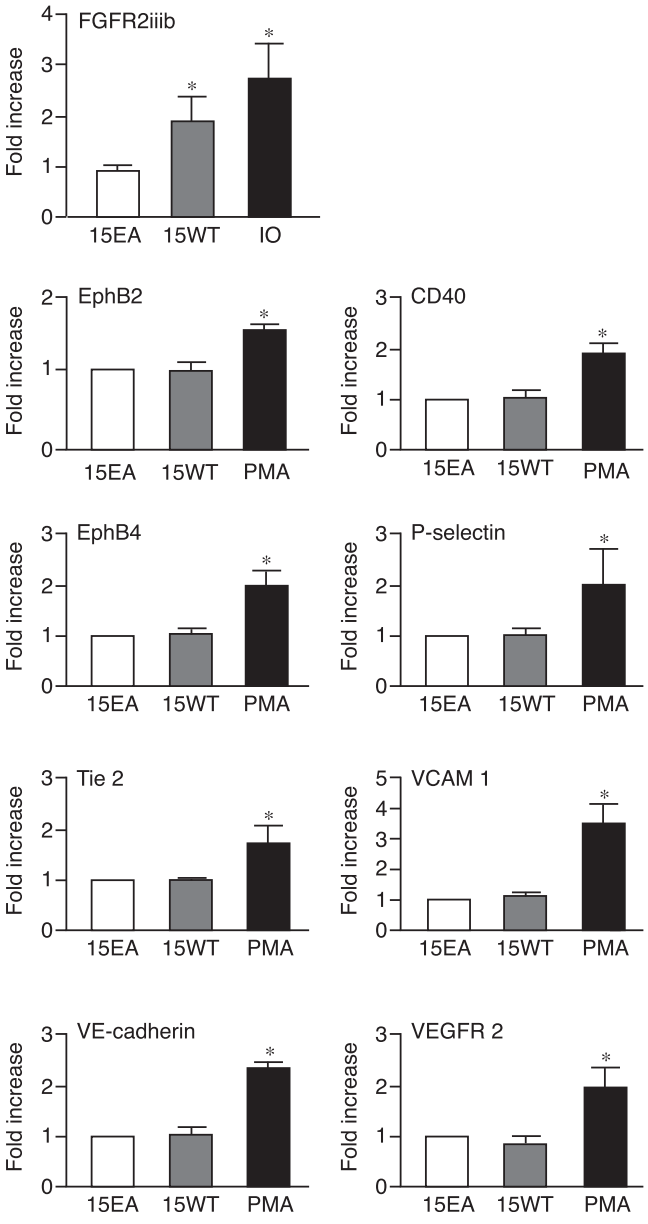

Figure 5. Ectodomain shedding of membrane receptors by overexpressed ADAM15 in "gain of function" cell-based assays. To identify potential substrates of ADAM15 that might be relevant for its function in pathological neovascularization, alkaline phosphatase (AP)-tagged membrane proteins with a known role in angiogenesis were overexpressed in mEFs together with WT mouse ADAM15 (15), or the catalytically inactive ADAM15E>A mutant (15EA). The graphs depict the relative AP-activity in the supernatant of the transfected cells, with the AP activity in cells transfected with a candidate substrate and the inactive ADAM15EA set to 1. Shedding of the substrate was confirmed by stimulating the transfected cells with either PMA to induce ADAM17-dependent shedding, or with ionomycin to induce ADAM10 and ADAM17 depending ectodomain processing. Each graph is representative of at least three separate experiments with two wells per experiment. These results demonstrate that overexpressed ADAM15 did not increase the shedding of any of the receptors tested here, with the FGFR2iiib serving as a positive control.

depletion of ADAM15 in endothelial cells decreased endothelial permeability and attenuated thrombin-induced barrier dysfunction, whereas overexpressing WT ADAM15 or ADAM15 E>A increased endothelial permeability and augmented the response to thrombin.[57] Overexpression of ADAM15 stimulated ERK phosphorylation independent of its catalytic activity, and the effect of ADAM15 or ADAM15E>A overexpression on the endothelial cell barrier could be reversed by inhibiting Src kinase.[18,57] These findings could help explain our observation that removing ADAM15 by targeted deletion in mice reduces pathological retinal neovascularization, whereas knocking in an inactivating point mutation in its catalytic site leads to an increase in pathological retinal neovascularization.

In summary, the catalytic activity of ADAM15 appears to be required for tumor development in a heterotopic tumor injection model, but not for pathological neovascularization in the mouse OIR model. The observation that ADAM15 showed very limited ectodomain shedding capability in our cell-based assays supports the notion that other domains of ADAM15 are more important for its role in OIR, such as regulating intracellular signaling pathways through previously established interactions with Src. Thus, this study helps to provide a better understanding of the role of the catalytic activity of ADAM15 in mice, which in turn is important for designing the proper strategy to block the function of ADAM15 for treatment of proliferative retinopathies such at retinopathy of prematurity, diabetic retinopathy, and the wet form of macular degeneration.

Acknowledgments

Supported by a National Institutes of Health grant from the Eye Institute (R01-EY015759 [CPB]). We thank Chingwen Yang from the Gene targeting facility at Rockefeller University (New York, NY, USA) for ES cell targeting; Willie Mark from the Memorial Sloan-Kettering Cancer Center (New York, NY, USA) for generating mice carrying a germline transmission of the targeted ADAM15 E>A allele; Viktoriya Nikolenko, Joshua Namm, and Elin Mogollon for excellent technical assistance and the staff of The Center for Laboratory Animal Services of the Hospital for Special Surgery for their help in taking care of these mice.

Disclosure: **T. Maretzky**, None; **C.P. Blobel**, None; **V. Guaiquil**, None

References

1. Friedlander M, Dorrell MI, Ritter MR, et al. Progenitor cells and retinal angiogenesis. *Angiogenesis*. 2007;10:89–101.
2. Bradley J, Ju M, Robinson GS. Combination therapy for the treatment of ocular neovascularization. *Angiogenesis*. 2007; 10:141–148.
3. Chen J, Smith LE. Retinopathy of prematurity. *Angiogenesis*. 2007;10:133–140.
4. Olsson AK, Dimberg A, Kreuger J, Claesson-Welsh L. VEGF receptor signalling - in control of vascular function. *Nat Rev Mol Cell Biol*. 2006;7:359–371.
5. Khong TL, Larsen H, Raatz Y, Paleolog E. Angiogenesis as a therapeutic target in arthritis: learning the lessons of the colorectal cancer experience. *Angiogenesis*. 2007;10:243–258.
6. Guaiquil VH, Swendeman S, Zhou W, et al. ADAM8 is a negative regulator of retinal neovascularization and of the growth of heterotopically injected tumor cells in mice. *J Mol Med*. 2010;88:497–505.
7. Guaiquil V, Swendeman S, Yoshida T, Chavala S, Campochiaro P, Blobel CP. ADAM9 is involved in pathological retinal neovascularization. *Mol Cell Biol*. 2009;29:2694–2703.
8. Horiuchi K, Weskamp G, Lum L, et al. Potential role for ADAM15 in pathological neovascularization in mice. *Mol Cell Biol*. 2003;23:5614–5624.
9. Weskamp G, Mendelson K, Swendeman S, et al. Pathological neovascularization is reduced by inactivation of ADAM17 in

endothelial cells but not in pericytes. *Circ Res*. 2010;106:932–940.

10. Guaiquil V, Swendeman S, Yoshida T, Chavala S, Campochiaro PA, Blobel CP. ADAM9 is involved in pathological retinal neovascularization. *Mol Cell Biol*. 2009;29:2694–2703.
11. Xie B, Shen J, Dong A, et al. An Adam15 amplification loop promotes vascular endothelial growth factor-induced ocular neovascularization. *FASEB J*. 2008;22:2775–2783.
12. Weskamp G, Mendelson K, Swendeman S, et al. Pathological neovascularization is reduced by inactivation of ADAM17 in endothelial cells but not in pericytes. *Circ Res*. 2010;106:932–940.
13. Komiya K, Enomoto H, Inoki I, et al. Expression of ADAM15 in rheumatoid synovium: up-regulation by vascular endothelial growth factor and possible implications for angiogenesis. *Arthritis Res Ther*. 2005;7:R1158–1173.
14. Bohm B, Aigner T, Roy B, Brodie TA, Blobel C, Burkhardt H. homeostatic effects of the metalloproteinase disintegrin ADAM15 in degenerative cartilage remodeling. *Arthritis Rheum*. 2005;52:1100–1109.
15. Charrier-Hisamuddin L, Laboisse CL, Merlin D. ADAM-15: a metalloprotease that mediates inflammation. *Faseb J*. 2008;22:641–653.
16. Najy AJ, Day KC, Day ML. ADAM15 supports prostate cancer metastasis by modulating tumor cell-endothelial cell interaction. *Cancer Res*. 2008;68:1092–1099.
17. Kuefer R, Day KC, Kleer CG, et al. ADAM15 disintegrin is associated with aggressive prostate and breast cancer disease. *Neoplasia*. 2006;8:319–329.
18. Sun C, Wu MH, Lee ES, Yuan SY. A disintegrin and metalloproteinase 15 contributes to atherosclerosis by mediating endothelial barrier dysfunction via Src family kinase activity. *Arterioscler Thromb Vasc Biol*. 2012;32:2444–2451.
19. Schonefuss A, Abety AN, Zamek J, Mauch C, Zigrino P. Role of ADAM-15 in wound healing and melanoma development. *Exp Dermatol*. 2012;21:437–442.
20. Blobel CP. Metalloprotease-disintegrins: links to cell adhesion and cleavage of TNF alpha and Notch. *Cell*. 1997;90:589–592.
21. Primakoff P, Myles DG. The ADAM gene family: surface proteins with adhesion and protease activity. *Trends Genet*. 2000;16:83–87.
22. Schlondorff J, Blobel CP. Metalloprotease-disintegrins: modular proteins capable of promoting cell-cell interactions and triggering signals by protein-ectodomain shedding. *J Cell Sci*. 1999;112(Pt 21);3603–3617.
23. Seals DF, Courtneidge SA. The ADAMs family of metalloproteases: multidomain proteins with multiple functions. *Genes Dev*. 2003;17:7–30.
24. Asakura M, Kitakaze M, Takashima S, et al. Cardiac hypertrophy is inhibited by antagonism of ADAM12 processing of HB-EGF: metalloproteinase inhibitors as a new therapy. *Nat Med*. 2002;8:35–40.
25. Black RA, Rauch CT, Kozlosky CJ, et al. A metalloproteinase disintegrin that releases tumour-necrosis factor-alpha from cells. *Nature*. 1997;385:729–733.
26. Condon TP, Flournoy S, Sawyer GJ, Baker BF, Kishimoto TK, Bennett CF. ADAM17 but not ADAM10 mediates tumor necrosis factor-alpha and L-selectin shedding from leukocyte membranes. *Antisense Nucleic Acid Drug Dev*. 2001;11:107–116.
27. Gutwein P, Mechtersheimer S, Riedle S, et al. ADAM10-mediated cleavage of L1 adhesion molecule at the cell surface and in released membrane vesicles. *FASEB J*. 2003;17:292–294.
28. Kurisaki T, Masuda A, Sudo K, et al. Phenotypic analysis of Meltrin alpha (ADAM12)-deficient mice: involvement of Meltrin alpha in adipogenesis and myogenesis. *Mol Cell Biol*. 2003;23:55–61.
29. Lieber T, Kidd S. Young MW. kuzbanian-mediated cleavage of Drosophila Notch. *Genes Dev*. 2002;16:209–221.
30. Moss ML, Jin SL, Milla ME, et al. Cloning of a disintegrin metalloproteinase that processes precursor tumour-necrosis factor-alpha. *Nature*. 1997;385:733–736.
31. Pan D, Rubin GM. Kuzbanian controls proteolytic processing of Notch and mediates lateral inhibition during Drosophila and vertebrate neurogenesis. *Cell*. 1997;90:271–280.
32. Qi H, Rand MD, Wu X, et al. Processing of the notch ligand delta by the metalloprotease Kuzbanian. *Science*. 1999;283:91–94.
33. Shirakabe K, Wakatsuki S, Kurisaki T, Fujisawa-Sehara A. Roles of Meltrin beta /ADAM19 in the processing of neuregulin. *J Biol Chem*. 2001;276:9352–9358.
34. Martin J, Eynstone LV, Davies M, Williams JD, Steadman R. The role of ADAM 15 in glomerular mesangial cell migration. *J Biol Chem*. 2002;277:33683–33689.
35. Maretzky T, Yang G, Ouerfelli O, et al. Characterization of the catalytic activity of the membrane-anchored metalloproteinase ADAM15 in cell-based assays. *Biochem J*. 2009;420:105–113.
36. Horiuchi K, Weskamp G, Lum L, et al. Potential role for ADAM15 in pathological neovascularization in mice. *Mol Cell Biol*. 2003;23:5614–5624.
37. Weskamp G, Cai H, Brodie TA, et al. Mice lacking the metalloprotease-disintegrin MDC9 (ADAM9) have no evident major abnormalities during development or adult life. *Mol Cell Biol*. 2002;22:1537–1544.
38. Smith LE, Wesolowski E, McLellan A, et al. Oxygen-induced retinopathy in the mouse. *Invest Ophthalmol Vis Sci*. 1994;35:101–111.
39. Hammes HP, Brownlee M, Jonczyk A, Sutter A, Preissner KT. Subcutaneous injection of a cyclic peptide antagonist of vitronectin receptor-type integrins inhibits retinal neovascularization. *Nat Med*. 1996;2:529–533.
40. Connor KM, Krah NM, Dennison RJ, et al. Quantification of oxygen-induced retinopathy in the mouse: a model of vessel loss, vessel regrowth and pathological angiogenesis. *Nat Protoc*. 2009;4:1565–1573.
41. Smith LE, Wesolowski E, McLellan A, et al. Oxygen-induced retinopathy in the mouse. *Invest Ophthalmol Vis Sci*. 1994;35:101–111.
42. Guaiquil VH, Hewing NJ, Chiang MF, Rosenblatt MI, Chan RV, Blobel CP. A murine model for retinopathy of prematurity identifies endothelial cell proliferation as a potential mechanism for plus disease. *Invest Ophthalmol Vis Sci*. 2013;54:5294–5302.
43. Sahin U, Weskamp G, Zheng Y, Chesneau V, Horiuchi K, Blobel CP. A sensitive method to monitor ectodomain shedding of ligands of the epidermal growth factor receptor. In: Patel TB, Bertics PJ (eds), *Epidermal Growth Factor: Methods and Protocols*. Totowa, NJ: Humana Press Inc.; 2006;99–113.
44. Swendeman S, Mendelson K, Weskamp G, et al. VEGF-A stimulates ADAM17-dependent shedding of VEGFR2 and crosstalk between VEGFR2 and ERK signaling. *Circ Res*. 2008;103:916–918.
45. Sahin U, Weskamp G, Zhou HM, et al. Distinct roles for ADAM10 and ADAM17 in ectodomain shedding of six EGFR-ligands. *J Cell Biol*. 2004;164:769–779.
46. Horiuchi K, Le Gall S, Schulte M, et al. Substrate selectivity of egf-receptor ligand sheddases and their regulation by phorbol esters and calcium influx. *Mol Biol Cell*. 2007;18:176–188.
47. Le Gall S, Bobe P, Reiss K, et al. ADAMs 10 and 17 represent differentially regulated components of a general shedding

Investigative Ophthalmology & Visual Science

machinery for membrane proteins such as TGFα, L-Selectin and TNFα. *Mol Biol Cell*. 2009;20:1785–1794.

48. Le Gall SM, Maretzky T, Issuree PDA, et al. ADAM17 is regulated by a rapid and reversible mechanism that controls access to its catalytic site. *J Cell Science*. 2010;123:3913–3922.
49. Peduto L, Reuter VE, Shaffer DR, Scher HI, Blobel CP. Critical function for ADAM9 in mouse prostate cancer. *Cancer Res*. 2005;65:9312–9319.
50. Blobel CP. ADAMs: key players in EGFR-signaling, development and disease. *Nat Rev Mol Cell Bio*. 2005;6:32–43.
51. Zheng Y, Schlondorff J, Blobel CP. Evidence for regulation of the tumor necrosis factor alpha -convertase (TACE) by protein-tyrosine phosphatase PTPH1. *J Biol Chem*. 2002;277:42463–42470.
52. Najy AJ, Day KC, Day ML. The ectodomain shedding of E-cadherin by ADAM15 supports ErbB receptor activation. *J Biol Chem*. 2008;283:18393–18401.
53. Howard L, Nelson KK, Maciewizc RA, Blobel CP. Interaction of the metalloprotease disintegrins MDC9 and MDC15 with two SH3 domain-containing proteins, endophilin I and SH3PX1. *J Biol Chem*. 1999;274:31693–31699.
54. Poghosyan Z, Robbins SM, Houslay MD, Webster A, Murphy G, Edwards DR. Phosphorylation-dependent interactions between ADAM15 cytoplasmic domain and Src family protein-tyrosine kinases. *J Biol Chem*. 2002;277:4999–5007.
55. Shimizu E, Yasui A, Matsuura K, Hijiya N, Higuchi Y, Yamamoto S. Structure and expression of the murine ADAM 15 gene and its splice variants, and difference of interaction between their cytoplasmic domains and Src family proteins. *Biochem Biophys Res Commun*. 2003;309:779–785.
56. Maretzky T, Le Gall SM, Worpenberg-Pietruk S, et al. Src stimulates fibroblast growth factor receptor-2 shedding by an ADAM15 splice variant linked to breast cancer. *Cancer Res*. 2009;69:4573–4576.
57. Sun C, Wu MH, Guo M, Day ML, Lee ES, Yuan SY. ADAM15 regulates endothelial permeability and neutrophil migration via Src/ERK1/2 signalling. *Cardiovasc Res*. 2010;87:348–355.

Investigative Ophthalmology & Visual Science